RESEARCH PAPER

CHANGE DETECTION OF VEGETATION COVER USING REMOTE SENSING AND GIS – A CASE STUDY OF THE WEST COAST REGION OF SOUTH AFRICA

Clive Coetzee[1]
[1]Faculty of Military Science, University of Stellenbosch, Private Bag X2, Saldanha, 7396, South Africa
***Corresponding author:** clivecoetzee@sun.ac.za
Received: June 14th, 2021 / Accepted: April 24th, 2022 / Published: June 30th, 2022
https://DOI-10.24057/2071-9388-2021-067

ABSTRACT. This article investigates the possible permanent vegetation cover (VC) change over an extended time for five municipal regions in South Africa by applying satellite-acquired remote sensed normalized difference vegetation index (NDVI) values within a geographic information system (GIS), spatial (West Coast District) and time (1981 to 2019 and 2000 to 2020) context. The NDVI index measures surface reflectance and give a quantitative estimation of vegetation growth and biomass. The study found relevance in its application since VC change detection has taken prominence over the past number of years in terms of sustainable development. Methods of analysis include image mapping, temporal image differencing, Moran I statistic, and the Mann-Kendall trend test. In the main areas that recorded significant changes in their NDVI values (plus or minus 0.4 difference on their original NDVI value) over time, in general, have experienced substantial and permanent VC change. These areas are also spatially clustered and concentrated within specific areas within the wider district. However, these areas constitute only a minority of areas (less than 20%), whereas most of the areas within the district did not experience such significant and permanent change in VC. Instead, the changes that did occur in these majority of areas were related to seasonal variation, i.e., temporal changes.

KEYWORDS: NDVI, NOAA, MODIS, vegetation cover, change detection

CITATION: Coetzee C. (2022). Change Detection of Vegetation Cover Using Remote Sensing and GIS – A Case Study of the West Coast Region of South Africa. Geography, Environment, Sustainability, 2(15), p. 91-102
https://DOI-10.24057/2071-9388-2021-067

Conflict of interests: The authors reported no potential conflict of interest.

INTRODUCTION

Vegetation Cover (VC) is most probably not a stable or constant phenomenon and presumably ebbs and flows over time. These changes could purely be seasonal or could be more permanent, i.e., the changes in VC may be short to medium term or could be long lasting. To this end, Alawamy et al. (2020) state that a great many of studies reveal that hardly any terrains on earth, in outlying places and isolated regions, are enduring in their unaffected environment.

VC change detection becomes very relevant when given the significance and relevance of VC change for economic development and planning and policy formulation. As Das and Angadi (2021) put it, "Exact statistics on how fast or slow VC transform and urban growth is crucial for the sustainable development and management of natural resources". This view is echoed by Alawamy et al. (2020) stating that our appreciation and mapping of VC change have preoccupied a relevant and significant bearing in policy-making in terms of the management of the world's natural resources as well as the monitoring of environmental changes.

It, therefore, seems plausible that the monitoring of VC change dynamics should be instrumental in the effectual planning and sustainable development of expanding economies. To this end, the NDVI is one of the more appropriate classification methods commonly adopted in exploring VC change (Aburas et al., 2015; Lunetta et al., 2006). Given that vegetation and, in particular, vegetation growth and biomass are in general regarded as the principal proxy of VC (Di Gregorio and Jansen 2000), the quantitative analysis regarding changes in its composition, biomass and vigour based on multispectral remote sensing assist in land cover change detection.

Remotely sensed NDVI features came to be extensively applied for VC change detection (for example, Mbatha and Xulu, 2018; Alphan and Derse, 2011; Cihlar, 2000). Rogan and Chen (2004) and Deng et al. (2008) described digital change detection as "the process of determining and/or describing changes in VC properties based on co-registered multi-temporal remote sensing data." Ayele et al. (2018) and Zhao et al. (2004) elaborate on the above statement proposing that the main focus of the change detection process based on digital images is to mathematicise the VC change for divergent features of interest for different time resolutions.

Gandhi et al. (2015) and Aburas et al. (2015) also note that the assessment of change detection is a desirable method of representing the changes detected in the various land use categories. The studies employed the NDVI technique with different threshold values for features extraction by calculating the percentage of land use per land cover and the associated change over time. Sahebjalal and Dashtekian (2013) detected the locations where the land cover has changed by subtracting the 2006 NDVI

image values from the 1990 NDVI image values. The derived 10% change threshold image, i.e., image displaying only the 10% decrease or increase in NDVI values, were presented.

According to Meneses-Tovar (2012), the NDVI can be used as a proxy for computing the difference between the energy received and emitted by earth phenomenon. The NDVI can be estimated by incorporating the Red and Near Infra-Red (NIR) bands of a sensor system, typically from Landsat satellites. The NDVI approach is based on the proposition that healthy/unhealthy vegetation has low/high reflectance rates of the electromagnetic spectrum's visible side. This is true because of the presence of high levels of chlorophyll. In addition to the above, Firl and Carter (2011) published a detailed tutorial on deriving Vegetation Indices (VI) from Landsat 5 Thematic Mapper and Landsat 7 Enhanced Thematic Mapper.

Given the fact that the NDVI index can be viewed as a dominant indicator that can be used in detecting the physical material at the surface of the earth over time intervals and in defined locations utilizing the remote sensing technique, the purpose (aim) of this study is to utilize the remote sensed NDVI over two periods (1982 to 2019 and 2000 to 2020) for five municipal regions located on the West Coast of South Africa as a change detection function to differentiate whether or not such changes have been permanent (long-lasting) in nature or not.

The article has been structured in the following way: Section 2 puts forward a brief background to calculating the NDVI, the study approach, the data generation process, and the study area. Section 3 focuses on the geographical information system (GIS), spatial, time, and trend analysis using the NDVI in point pattern methodology. Reconciling the findings of the vegetation temporal change analysis is the focus of Section 4. In the final section, a summary and conclusion are provided.

MATERIALS AND METHODS

Study Area

Five municipal regions were chosen for this study. There are no particular reasons for this choice, and it is purely by default. These five municipal regions are:

Swartland (size = 3 700 km^2)
Bergriver (size = 2 015 km^2)
Saldanha Bay (size = 4 407 km^2)
Cederberg (size = 8 007 km^2)
Matzikama (size = 12 981 km^2)

The municipal regions (right panel) within the South African context (left panel) are displayed in Figure 1. The district (municipalities as a collective) are located on the West Coast of South Africa within the Western Cape Province (red boundary).

The district is bordered by the Atlantic Ocean on the west and the Swartland region on the east. As such, the district is characterised by a low winter rainfall which decreases rapidly northwards, from 400 mm in the Swartland region to less than 100 mm in the Matzikama region. Because of dry summers, the Region has a distinct vegetation of grasses, shrubs, and trees. As part of the Cape Floral Kingdom, the Region is home to thousands of species of plants, including fynbos which is indigenous to the Region and found nowhere else in the world.

Overall, the Regional climate is typically Mediterranean, with warm, dry summers and mild, wet winters and low summer rainfall prevail. Near the coast, summer's temperature rises from a pleasant low of 15° C to a heart warming 27° C. Inland temperatures are some 3-5° C higher. Coastal winters see the mercury dropping to a mild 7° C at night and rising to a comfortable 18° C by day. Away from the beach, morning wakens to an invigorating 5° C and midday peaks at 22° C. Because of the Indian and Atlantic oceans' influence, inland and coastal temperatures differ over short distances, and macro- and micro climates are created.

Methods

According to Wu et al. (2016) and Zhang et al. (2013), NDVI can be used as a measure or proxy of surface reflectance and offer a quantitative estimation of vegetation health, i.e., vegetation growth and biomass. In general, healthy vegetation (greater levels of chlorophyll) reflects greater levels of near-infrared (NIR) and green light in relation to other wavelengths. However, greater levels

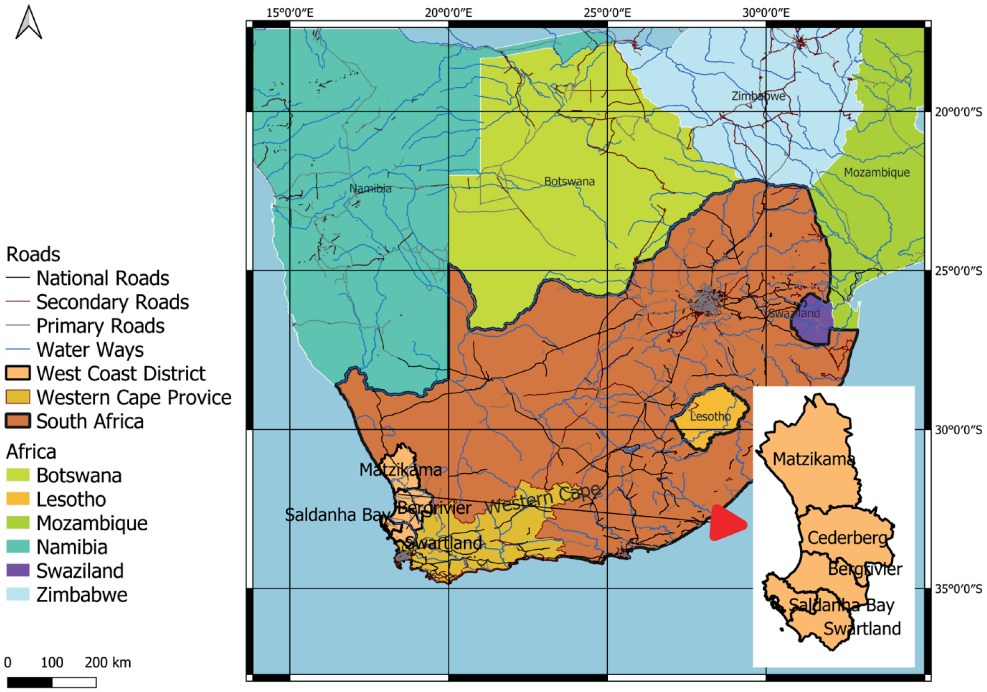

Fig. 1. Regions with the South African Context

of red and blue light (RED) are absorbed. A plant is green as observed by the human eye, since the chlorophyll pigment in it reflects the green waves and absorbs the red waves. Consequently, a healthy/unhealthy plant - one with many/few chlorophyll and cell structures - actively absorbs/reflects red light and reflects/absorbs NIR. The exact opposite will be true for an unhealthy plant. To this end space-based satellite sensors measure wavelengths of light absorbed and reflected by green plants.

The index defined values ranges from -1.0 to 1.0, portraying greens, where negative values are mainly formed from clouds, water and snow, and values close to zero are primarily formed from rocks and bare soil. Values 0.1 or less match empty areas of rocks, sand or snow. Values between 0.2 to 0.4 represent shrubs and meadows, while values ranging from 0.6 to 0.8 represent temperate and tropical forests (Wu et al., 2016; Zhang et al., 2013).

The NDVI derived values per location will be presented analyzed in a Geographical Information System (GIS) context. Visualizing the NDVI values gives a perspective of the state of vegetation cover in the Region and notably the historical trend and changes thereof at a very decentralized level. In the main, the analysis was performed in Excel, EVIEWS, and QGIS.

To test or assess the possible prevalence of spatial autocorrelation the study employed the Global Moran I index. According to Sowunmi et al. (2012), the global spatial autocorrelation (Moran I) analysis supply applicable statistics to capture the sequence of NDVI values in the Region of interest. Homogeneity of the Region of interest (the locations displays the same NDVI patterns) were assumed. Spatial clustering of similar values across geo-space are associated with positive Moran I values. Negative and significant values proposes that neighbouring values are more distinct than expected by chance. This suggest that high values are often found near low values. An advantage of using the Moran I is that its maximum and minimum possible values are not forced within the (–1, 1) range, unlike the Pearson product-moment correlation coefficient, for example. The Moran's I can be calculated as follows(Viton, 2010);

$$I = \left(S / \sum ijwij\right)\left(\frac{\sum ujwij(b_1 - b)(b_j - b)}{\sum i(bi - b)^2}\right) \quad (1)$$

where
S = number of observations
Σijwij= sum over all *i* and *j* of *ωij*
wij = spatial weight between *i* and *j*.
ωij bibj = weight * cross product terms.

To further explore the possible spatial autocorrelation nature of the locations, the study made use of a local indicator of spatial association (LISA) suggested in Anselin (1995). A LISA is seen as having two important characteristics. First, it provides a statistic for each location with an assessment of significance. Second, it establishes a proportional relationship between the sum of the local statistics and a corresponding global statistic. These statistics and relationships are then presented in the form of a cluster map and a significance map. The significance map shows the locations with a significant local statistic, with the degree of significance reflected in increasingly darker shades of green. The cluster map augments the significant locations with an indication of the type of spatial association, based on the location of the value and its spatial lag in the Moran scatter plot.

Following on the possible spatial autocorrelation nature of the locations, the study tested the NDVI behaviour of each location for the existence of possible structural breaks. A structural break occurs when a time series abruptly changes at a point in time and, as such, proposes a fundamental change in the underlying vegetation cover. In time series analysis, the detection of structural breaks can be performed using the cross-section independent and cross-section dependent unit root testing methods. The Dickey-Fuller test has been widely used to detect possible structural breaks and, as such, has been used as well. The presence of a unit root (structural break) in the NDVI of a location or locations suggests that the vegetation cover has indeed fundamentally changed at that location or locations. The testing procedure for the Dickey-Fuller test is applied to the model, i.e.,

$$\Delta y_t = a + \beta_t + \gamma y_{t-1} + \delta_1 \Delta y_{t-1} + \ldots + \delta_{p-1} \Delta y_{t-p+1} + \varepsilon_t \quad (2)$$

where
α = constant term
β = the coefficient on a time trend
ρ = the lag order of the autoregressive process
y = variable under consideration
ε = error term

Supplementing the structural break analysis, the study also employed a trend assessment of the NDVI behaviour of each location. In this regard, the Mann Kendall Trend Test was used to analyze the NDVI behaviour of each location for consistently increasing or decreasing trends. The Mann-Kendall test is used to determine whether a time series has a monotonic upward or downward trend. A mean-reverting NDVI series (irrespective of location) suggest very little, if any, change in the underlying vegetation cover over the period under consideration. However, a mean-reverting series excludes the presence of any significant trend (either upward or downward). Thus, the presence of a trend proposes that the underlying vegetation cover has indeed changed over the period under consideration. The Mann Kendall Trend Test is applied to the model, i.e.,

$$s = \sum_{k=1}^{n-1} \sum_{j=k+1}^{n} \operatorname{sgn}\left(x_j - x_k\right) \quad (3)$$

where
Time Series = *x1, .., xn*
n = length of the sample
xk and *xj* are from k=1, 2, …, *n-1* and *j= k+1*, …, n

$$sgn\left(xj - xk\right) = \begin{cases} +1, if\,(xj - xk) \rangle 0 \\ 0, if\,(xj - xk) = 0 \\ -1, if\,(xj - xk) \langle 0 \end{cases} \quad (4)$$

Data

This study used two remote sensing datasets in both the general and specific approaches. The first dataset is the NOAA CDR AVHRR NDVI: Normalized Difference Vegetation Index, Version 5 dataset (NOAA, 2021 and Vermote et al., 2014). The dataset is available from 1981-06-24 to 2021-03-04 on a daily basis, gridded at a resolution of 0.05°, computed globally over land surfaces and provided by NOAA (NOAA, 2020). The data is generated using the Google Earth Engine Code Editor.

The second dataset is the MOD13Q1.006 Terra Vegetation Indices 16-Day Global 250 m dataset (MODIS, 2021). The data is available from 2000-02-18 to 2021-02-18, twice monthly, gridded at 250 m spatial resolution (pixel size), and provided by NASA LP DAAC at the USGS EROS Centre (USGS, 2020 The data is also generated using the Google Earth Engine Code Editor.

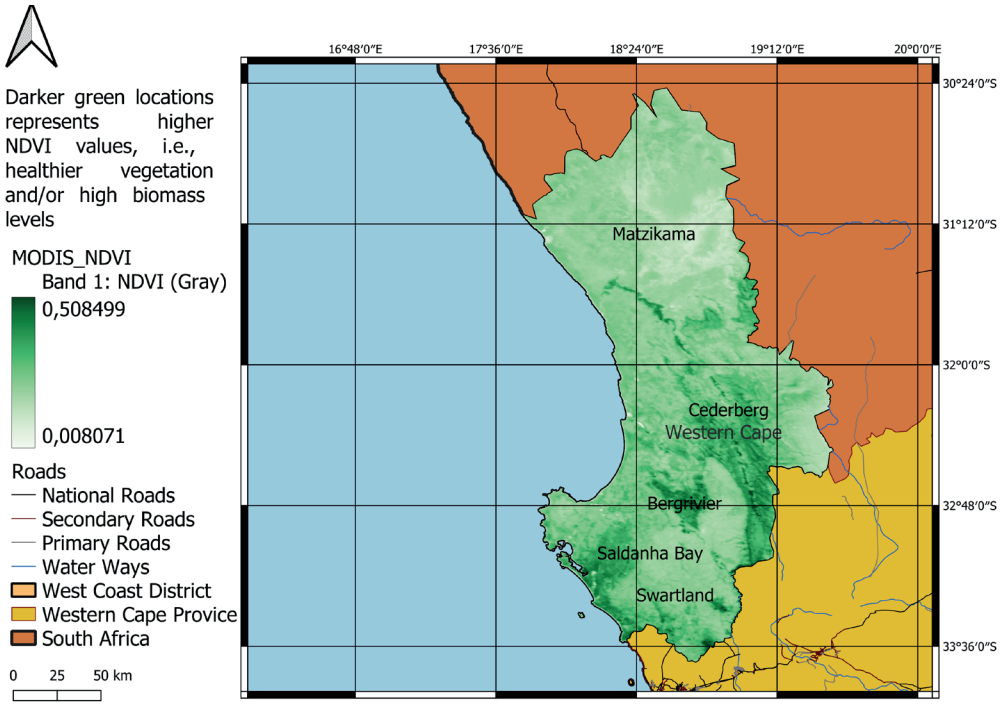

Fig. 2. NOAA and MODIS NDVI Map

The results of the data generation process (both datasets) can be presented as shown in Figure 2. The figure to the left represents the daily average (1981 to 2019) NOAA NDVI value for the district (five regions collective) per granular location, whilst the right figure represents the daily average (2000 to 2020) USGS MODIS NDVI value for the district also per granular level. In both cases, dark green coloured locations represent NDVI values closer to 1, whilst very light green (almost white) coloured locations represent NDVI values closer to 0. As referenced, locations with high NDVI values portray healthy vegetation and/or high biomass levels and vice versa.

Given the size of the district, the study will also make use of point pattern analysis. Therefore, it was necessary to generate random points within each of the regions. The random points in the polygons function in QGIS were used to generate 100 random point-locations in each Region of interest, i.e., 500 point-locations in total. These randomly generated 500 point-locations are displayed in Figure 3. It is relevant to note that some areas were not covered with random points suggesting that the included random points may not be fully representative of the Region as a collective. However, it is worth noting that these areas are mostly nature reserves or high elevation areas, which should, in theory, be relatively immune to significant and permanent vegetation change.

These 500 point-locations were populated with monthly NDVI data from 1981 to 2019 using the NOAA dataset and from 2000 to 2020 using the MODIS dataset using the Google Earth Engine Code Editor. In terms of the two datasets, the following general statistics were presented:

NOAA dataset, 500 point-locations and 448 months (224 000 observations)

MODIS dataset, 500 point-locations and 251 months (125 500 observations)

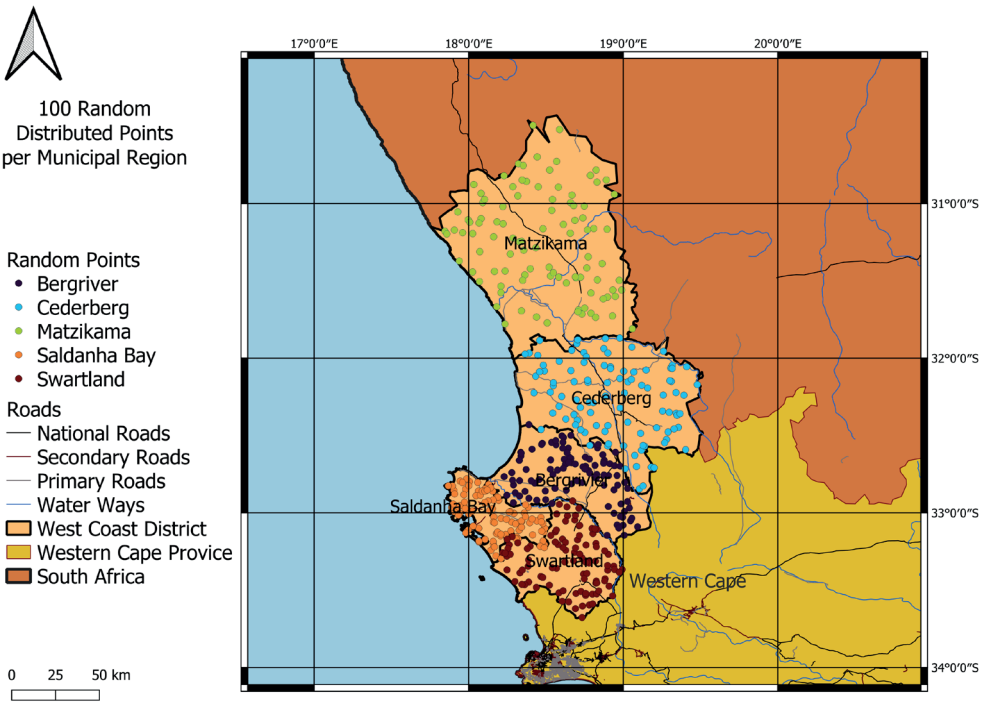

Fig. 3. Random Point-locations

Results - NDVI GIS Analysis

The NOAA and MODIS datasets for the 500 point-locations for the stated periods is presented in panel format in Figure 4 and Figure 5. The mean regional (RegionDemean) and mean district (Regionmean) NDVI values for the NOAA and MODIS datasets are illustrated with the red and green lines, respectively. Point-locations 0 to 44 802, 44 903 to 89 601, 89 602 to 134 401, 134 402 to 179201 and 179 201 to 224 000, represent the Bergriver, Cederberg, Matzikama, Saldanha Bay and Swartland regions with regards to the NOAA dataset, respectively. Point-locations 0 to 25 101, 25 102 to 50 201, 50 202 to 75 301, 75 302 to 100 401 and 100 402 to 125 500, represent the Bergriver, Cederberg, Matzikama, Saldanha Bay and Swartland regions with regards to the MODIS dataset, respectively.

From a time perspective, the two datasets can be presented as set out in Figure 6 and Figure 7. The datasets indicate the monthly NDVI value per point-location (500 point-locations) for the respective periods. The colored lines represenstthe various point locations and given the number of the locations it is not possible to present them in a legend. The seasonal nature of the NDVI values is clearly visible. In general, the datasets seem to contain no significant structural breaks, i.e., fairly constant mean values following a seasonal trend.

Figure 8 displays the temporal difference image (in absolute format) between the average February 2019, 2018, and 2017 and February 1982, 1983, and 1984 NDVI values in terms of the NOAA dataset (left panel) and the temporal difference image (in absolute format) between the average February 2020,2019 and 2018 and February 2000, 2001 and 2002 NDVI values in terms of the MODIS dataset (right panel). Dark green represents significant positive change (increase in NDVI values). In contrast, white represents significant negative change (decrease in NDVI values), suggesting that many locations within the Swartland, Saldanha Bay, and Bergriver regions experienced positive change while most locations with the Cederberg and Matzikama regions experienced negative change.

The global spatial autocorrelation (Moran I) analysis results for the February 1982 and February 2018 periods regarding the NOAA dataset and February 2000 and February 2020 periods concerning the MODIS dataset are displayed in Figure 9 and Figure 10. The Moral I statistics are displayed in the first column showing a value of 0.74

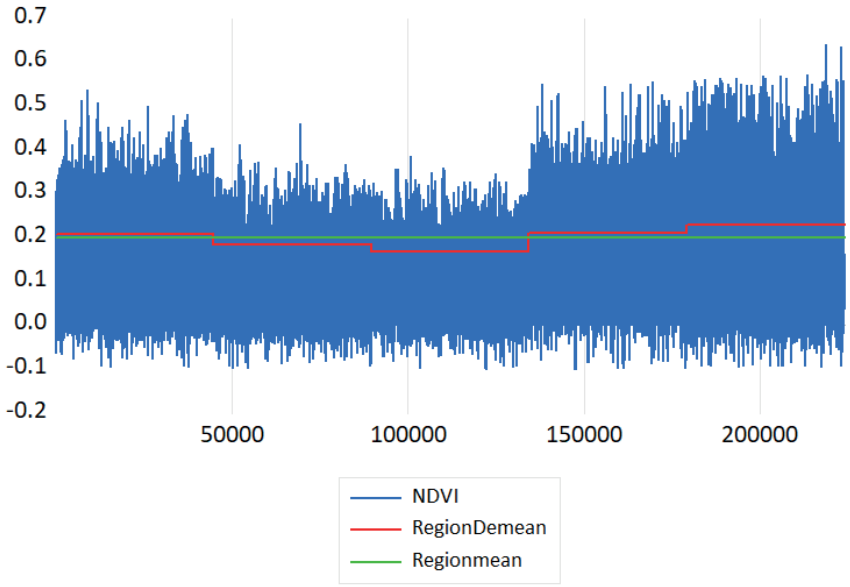

Fig. 4. NOAA NDVI per Point-Location, January 1982 to April 2019

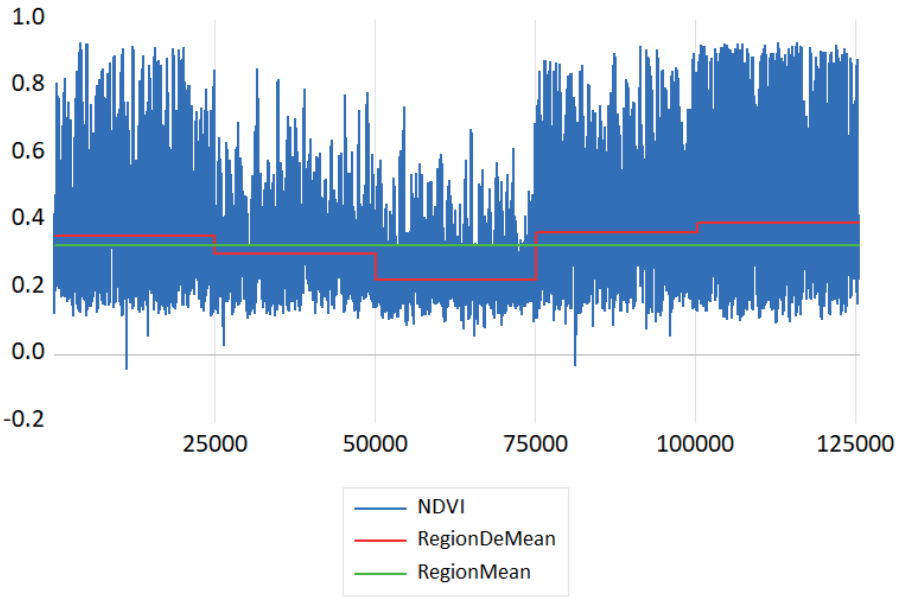

Fig. 5. MODIS NDVI per Point-Location, January 2000 to December 2020

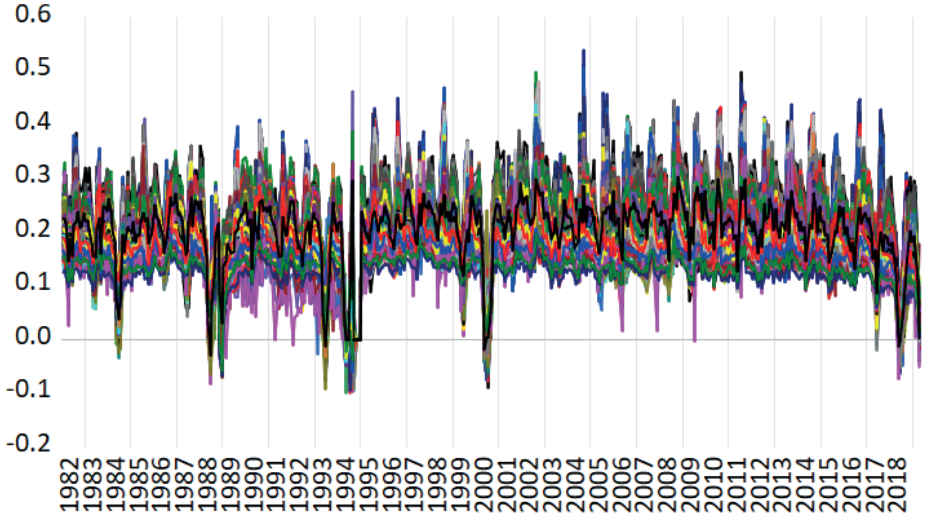

Fig. 6. NOAA NDVI per Month, January 1982 to April 2019

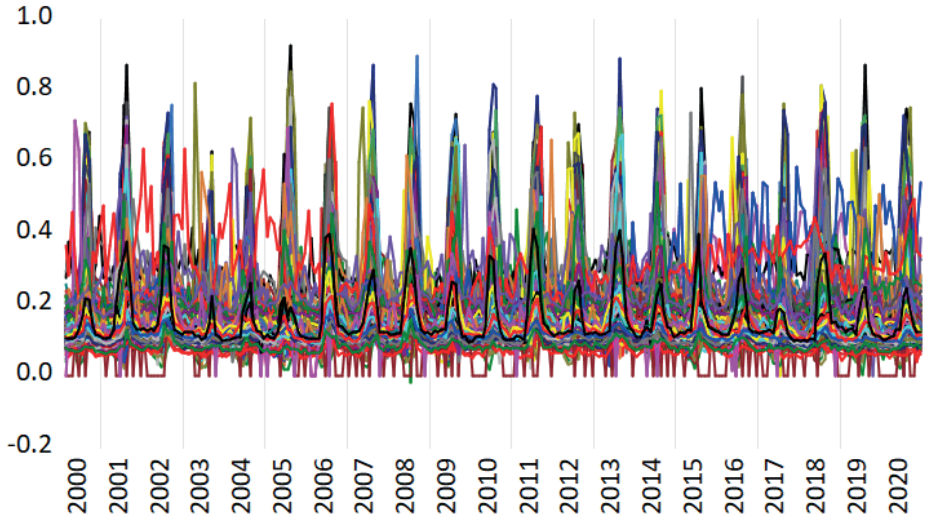

Fig. 7. MODIS NDVI per Month, January 2000 to December 2020

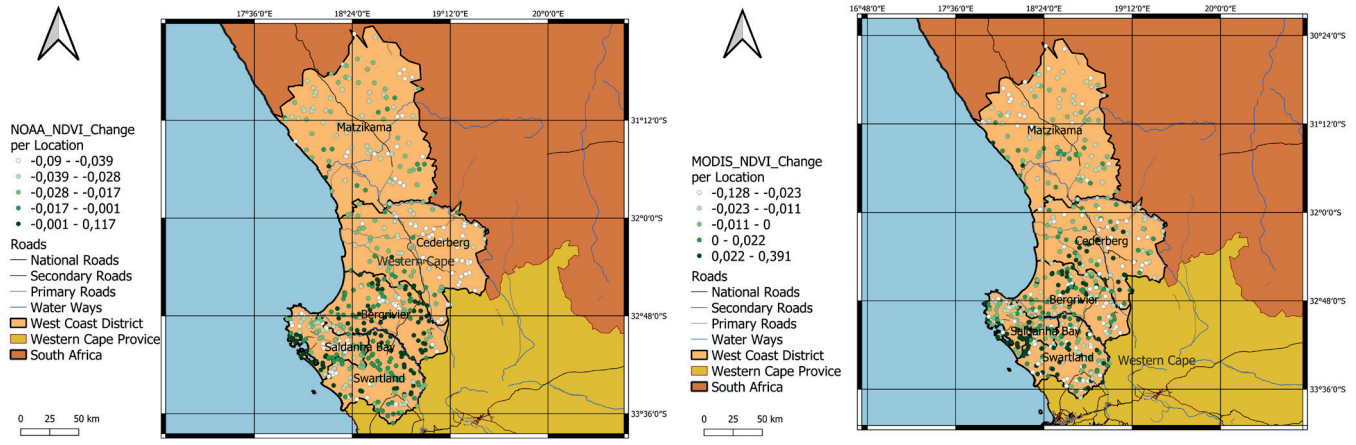

Fig. 8. NOAA and MODIS NDVI Change Visualization

and 0.73 in February 1982 and February 2018, respectively, regarding the NOAA dataset, compared to 0.39 and 0.51 in February 2000 and February 2020 regarding the MODIS dataset. The associated z-values (not indicated) for the four periods suggest a strong acceptance of the alternative hypothesis of spatial clustering. The second column (cluster map) shows that the high NDVI locations bordered by high NDVI locations (high-high clusters in red) are concentrated in the six sub-point-locations (representing around 24 percent of the 500 point-locations). The low-low NDVI point-locations (low-low clusters in blue) are concentrated in the four sub-point-locations (representing about 20 percent of the 500 point-locations). The results (as per the third column = significance map) also show that the NDVI point-locations have not changed much over the two respective periods, irrespective of the dataset, i.e., the point-locations with significant clusters (in green) have not changed over the two periods, regardless of any dataset.

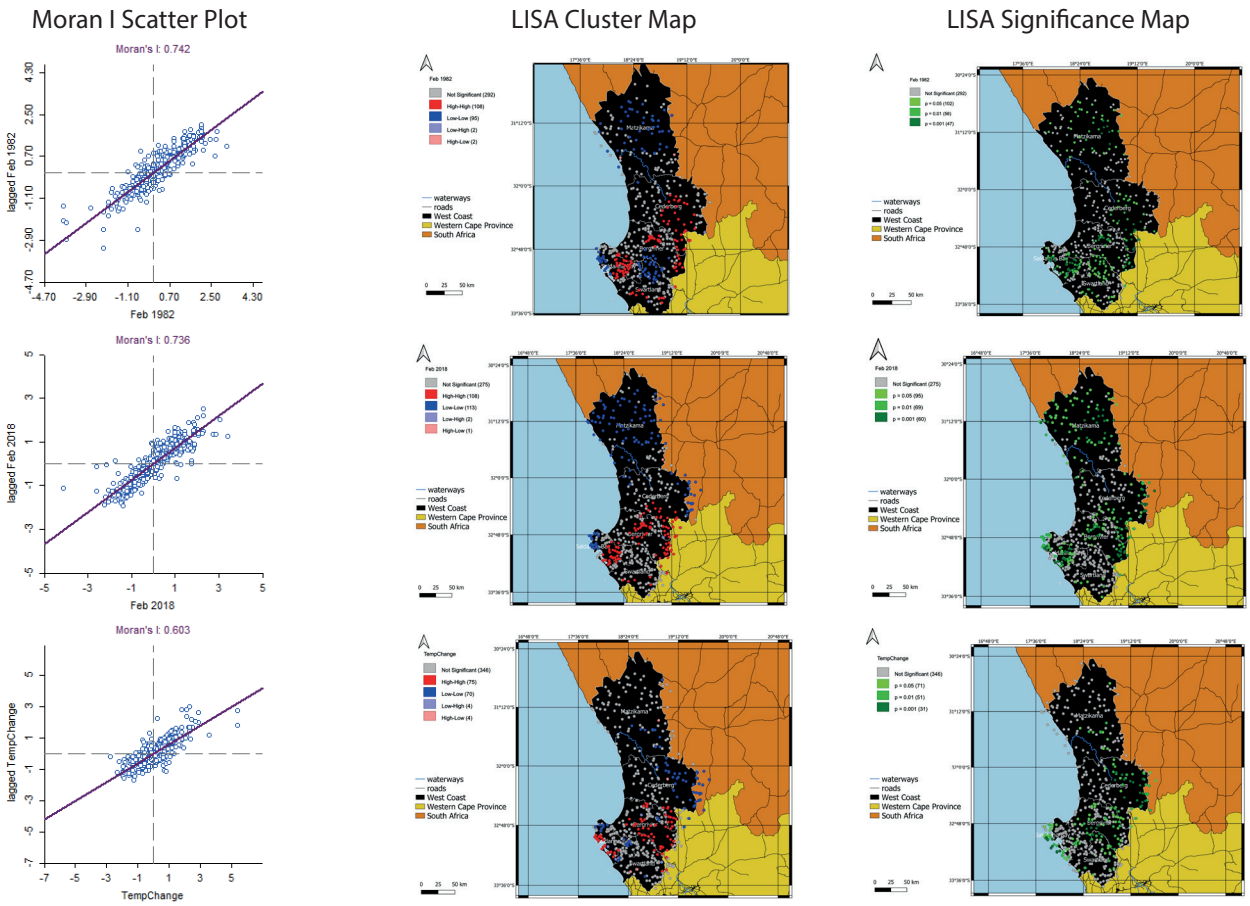

Fig. 9. Moran I, Cluster and Significance Map, February 1982 and 2018 and February 1982 to 2018 (change) NDVI values, NOAA dataset

Note: top row = February 1982, Middle row = February 2018 and Bottom row = February 2018 minus February 1982 (change)

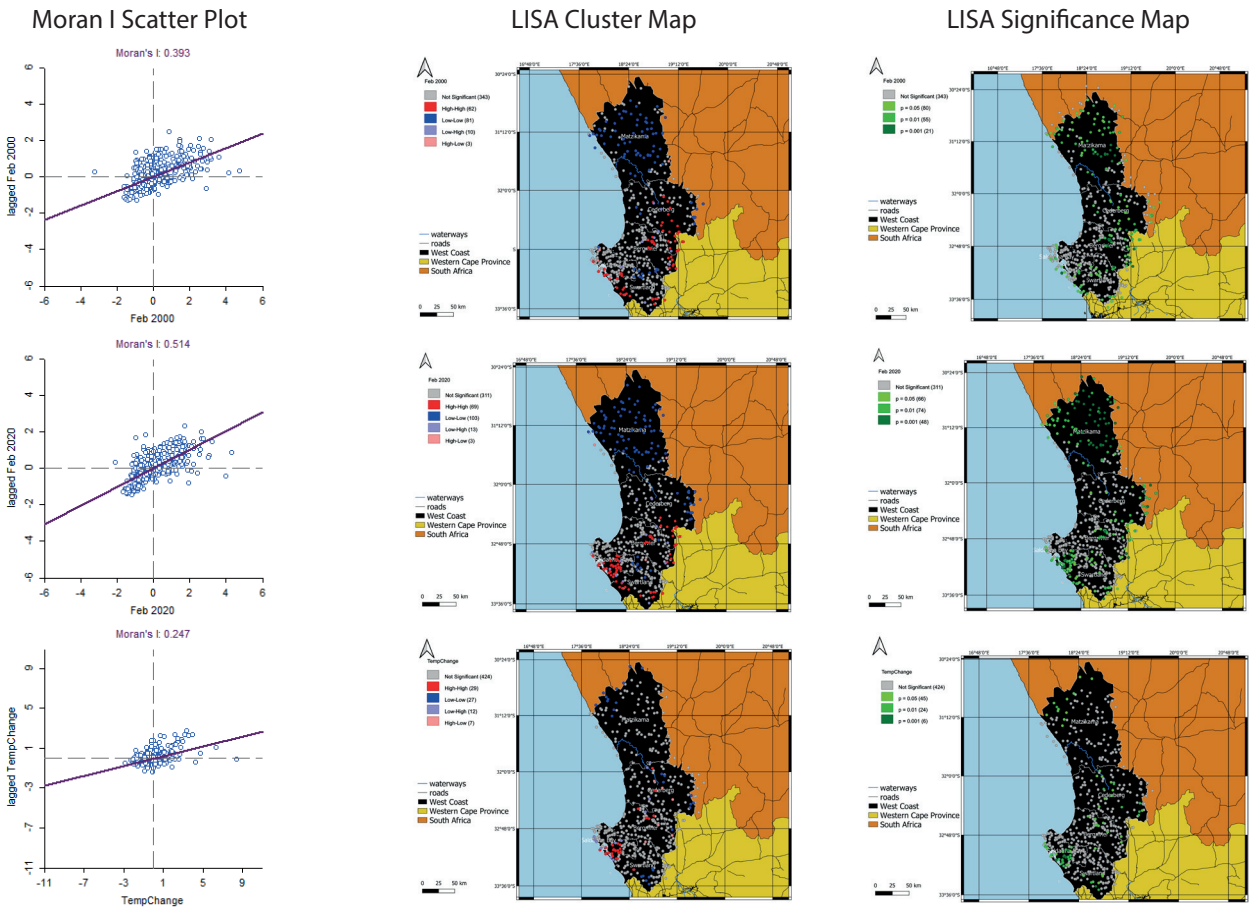

Fig. 10. Moran I, Cluster and Significance Map, February 2000 and 2020 and February 2000 to 2020 (change) NDVI values, NOAA dataset

Note: top row = February 2000, Middle row = February 2020 and Bottom row = February 2020 minus February 2000 (change)

Additionally, the Moran I analysis (Figure 11) displays the average monthly Moran I statistics for the year 1982 (grey line) and 2018 (yellow line) using the NOAA dataset and the average monthly Moran I statistics for the year 2000 (orange line) and 2020 (blue line) using the MODIS dataset. It is noticeable that the Moran I statistics significantly increases during the winter (rain) months irrespective of the dataset. In each case the Moran I statistics doubles during the winter months. The spatial autocorrelation of the 500 point-locations, therefore, displays significant seasonal patterns.

The Moran I derived results suggest strong spatial relationships, especially during the winter months (May to August). Testing for the presence of time relationships (figures 6 and 7) also seems warranted (structural break analysis) utilizing both the cross-section independent and cross-section dependent unit root testing procedures in EViews (Chang and Song 2002). The results (not presented) for both datasets strongly support the stationarity hypothesis in that the various test statistics' (Levin, Lin & Chu, Pesaran, and Shin, ADF – Fisher, PP – Fisher, Bai and Ng, Pooled statistic, CIPS, and Truncated CIPS) probability values indicate the acceptance of the alternative hypothesis, i.e., the absence of unit-roots. This suggests that the NDVI values of the 500 point-locations are mean-reverting over time, and therefore no significant structural change has occurred.

However, on closer inspection of the results, there are indeed point-locations that experienced structural breaks over the period. Thus, although the vast majority of point-locations have experienced no significant change (mean-reverting), there are indeed several point-locations that have (contain unit-roots). Regarding the NOAA (left panel) and MODIS (right panel) datasets, there are 197 and 139 point-locations (of the 500 point-locations) where the null hypothesis, i.e., the presence of unit roots, could not be rejected. These point-locations (unit root point-locations) are displayed in Figure 12 below (red colour).

Identifying a trend in a series, albeit including a seasonal component, can be done by applying a nonparametric test such as the Mann-Kendall trend test (Mbatha and Xulu, 2018; Drapela and Drapelova, 2011). Meals et al. (2011) further state that the Mann-Kendall trend test is especially appropriate for non-normal distribution data, which is the case for both datasets (applying the Jarque-Bera and Shapiro-Wilk tests to both datasets reveal that none of the point- locations or months are normally distributed, test results not included). Meals et al. (2011) further argue that the Mann-Kendall test explores whether increases or decreases in the y-values over time can be found. This can be done through what is essentially a nonparametric form of monotonic-trend regression analysis. The Mann-Kendall test assesses the sign of the post-measured and pre-measured data difference. Each post-measured value is compared to all values measured earlier; resulting in a total of n(n-1)/2 possible pairs of data. In this case, the aggregate observations are represented by n. This argument is supported by Ahmad et al. (2015) that further argue that the Mann-Kendall test is also not affected by outliers.

There has been no trend over time accounts for the null hypothesis (H0), while there has been a trend (increasing or decreasing) over time accounts for the alternate hypothesis (H1) (Motiee and McBean, 2009). Measuring the significance of the trend is done through the test statistic Zs. In other words, if | Zs| is greater than Zα/2, then the alternative hypothesis is valid, implying that the trend is not significant. The chosen level of significance (e.g. 5% with Z 0.025 = 1.96) is represented by α. An additional statistic obtained performing the Mann-Kendall test is Kendall's tau. Kendall's tau measures correlation and hence accounts for the significance of the association between the two variables. Kendall's tau is performed on the data ranks, i.e., the values are put in order and numbered, 1 for the lowest value, etc. Like other correlation measures, Kendall's tau assumes values between ±1 and +1, with a positive correlation indicating that the ranks of both variables increase or decrease together and vice versa (Yue and Wan 2004).

Concerning the NOAA and MODIS datasets, there were on average 367 and 171 point-locations (of the 500 point-locations) where the alternative hypothesis could not be rejected. These point-locations (trend point-locations) are displayed in Figure 13 below (red colour). Within the NOAA dataset (left panel), most trend point-locations are within the Bergriver and Swartland regions. Within the MODIS dataset (right panel), most trend point-locations are within the Cederberg and Bergiver regions. Again, it is evident that the two types of point-locations (non-trend in green and trend in red) follow a spatial clustering pattern. Therefore, the trend point-locations are characterized by spatial and time autocorrelation, while the non-trend point-locations are represented by only spatial autocorrelation.

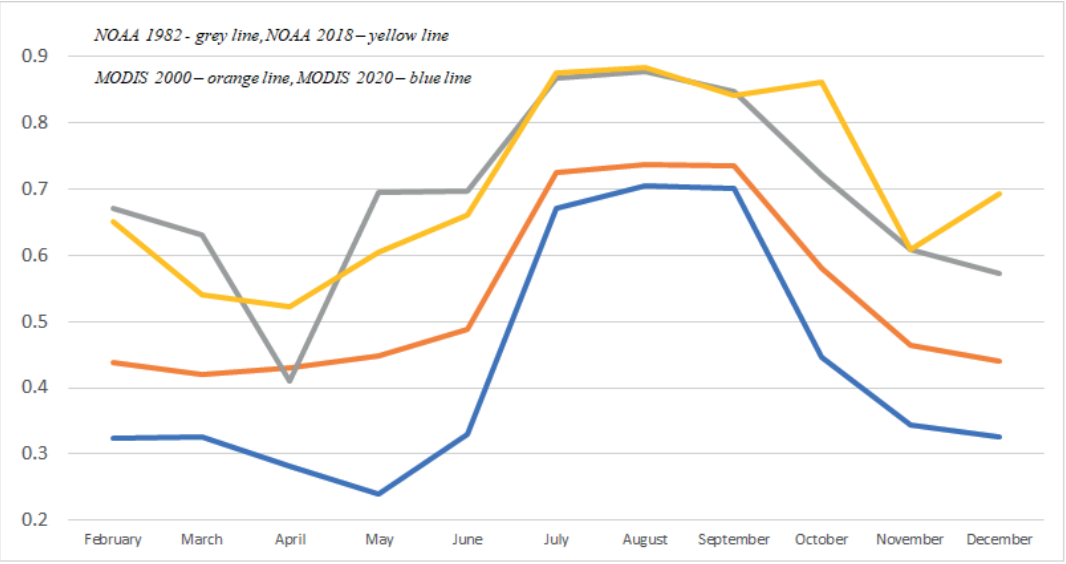

Fig. 11. Average Monthly Moran I statistics for the selected years using the NOOA and MODIS datasets

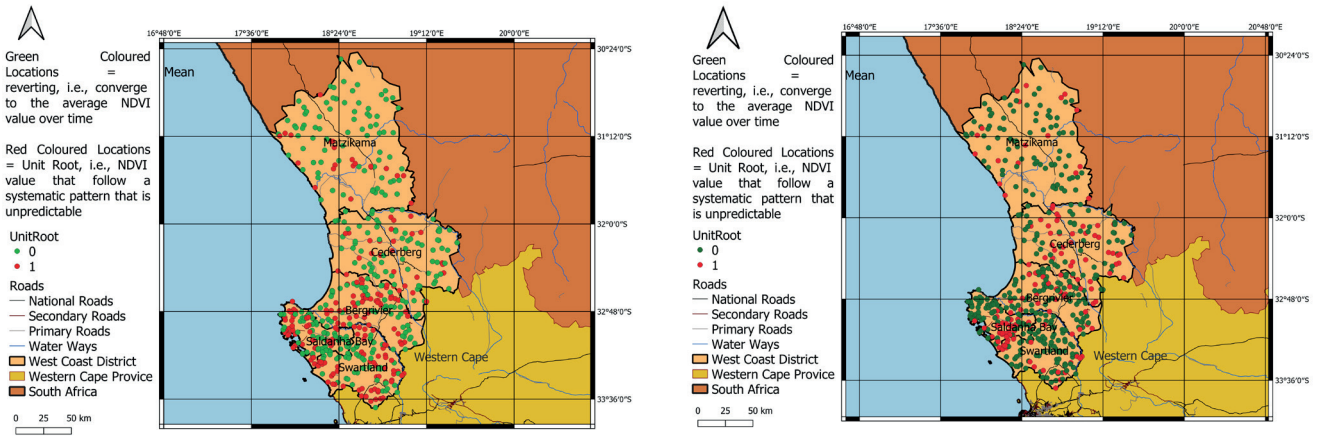

Fig. 12. Mean Reverting and Unit Root Point-locations

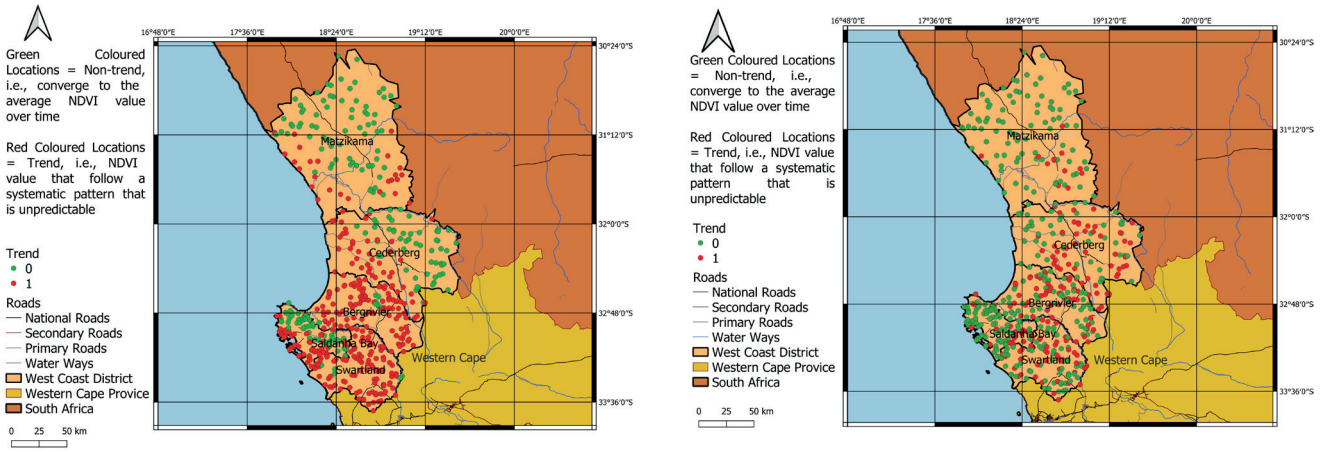

Fig. 13. Non-trend and Trend Point-locations

DISCUSSION

Aligning the findings of the time autocorrelation analysis (Figure 12) and the trend analysis (Figure 13) yields the results as presented in Figure 14. The results were derived from averaging the NOAA and MODIS structural break and trend images. The point-locations with structural breaks and trends are shown in red, while the mean-reverting and non-trend point-locations are shown in green. The spatial autocorrelation or spatial clustering is again very evident. It is also apparent that most areas or point-locations within the district did not experience any significant trend/structural change in vegetation over the 40- or 20-year periods. Thus, it can be argued that the majority of the vegetation change was most probably because of seasonal variation and changes thereof. Locating the structural break and trend -point-locations, i.e., point-locations that experienced statistically significant vegetation change over time within the NOAA and MODIS temporal differencing images (Figure 3.5), yields the results in Figure 15. Within the average NOAA and MODIS temporal differencing image, only point-locations that recorded significant NDVI change (increase or decrease of more than 0.4 in the original NDVI value) have been highlighted, i.e., blue coloured point-locations (left image) and bright coloured point-locations (right image). In the main areas that recorded significant changes in their NDVI values (plus or minus 0.4 difference on their original NDVI value) over time, in general, have experienced significant and permanent vegetation change. These areas are also spatially clustered and concentrated within specific areas within the wider district. However, these areas constitute only a minority of areas (less than 20%), whereas most of the areas within the district did not experience such significant and permanent change in vegetation. Instead, the changes that did occur in these majority of areas were related to seasonal variation, i.e., temporal changes. It is, therefore, possible to argue that most of the point-locations within the district have not experienced any significant and permanent change since the 1980'

In the main areas that recorded significant changes in their NDVI values (plus or minus 0.4 difference on their original NDVI value) over time, in general, have experienced significant and permanent VC change. These areas are also spatially clustered and concentrated within specific areas within the wider district. These areas constitute, however, only a minority of areas (less than 20%), whereas most of the areas within the district did not experience such significant and permanent change in VC. Rather, the changes that did occur in these majority of areas were related to seasonal variation, i.e., temporal changes. It is, therefore, possible to argue that most of the point-locations within the district have not experienced any significant and permanent change since the 1980s.

For the purpose of this article, no inference will be made as to the causes for the significant and permanent VC change. For such an inference, further work will be required, which falls outside the scope of this article. Nevertheless, various hypothetical causes can be put forward, such as Agricultural expansion, Urban expansion, Surface water change, and change in weather patterns. Le Roux, Cooper, and Mans (2016) argued that proximate causes for Land Use Land Cover Change in the Western Cape Province (the West Coast Region falls within the Western Cape Province, see Figure 2.1) were identified as infrastructure, agriculture and forestry changes and underlying causes as political, demographic, economic, technological and cultural factors.

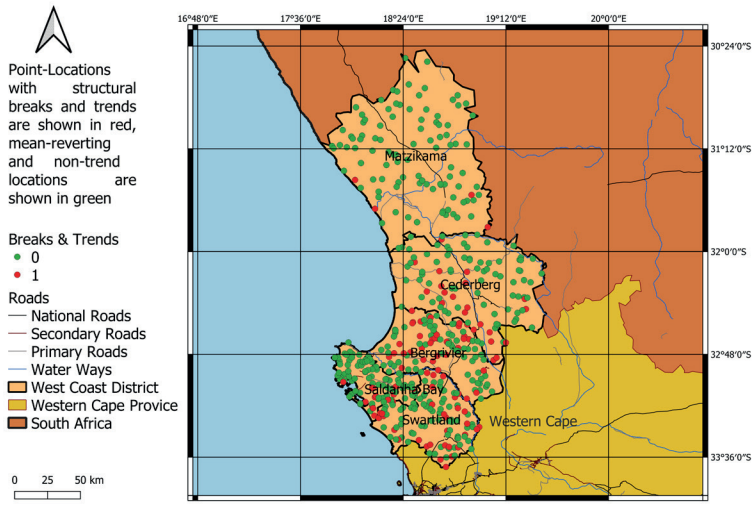

Fig. 14. Non-Change vs Change Vegetation Cover Point-locations

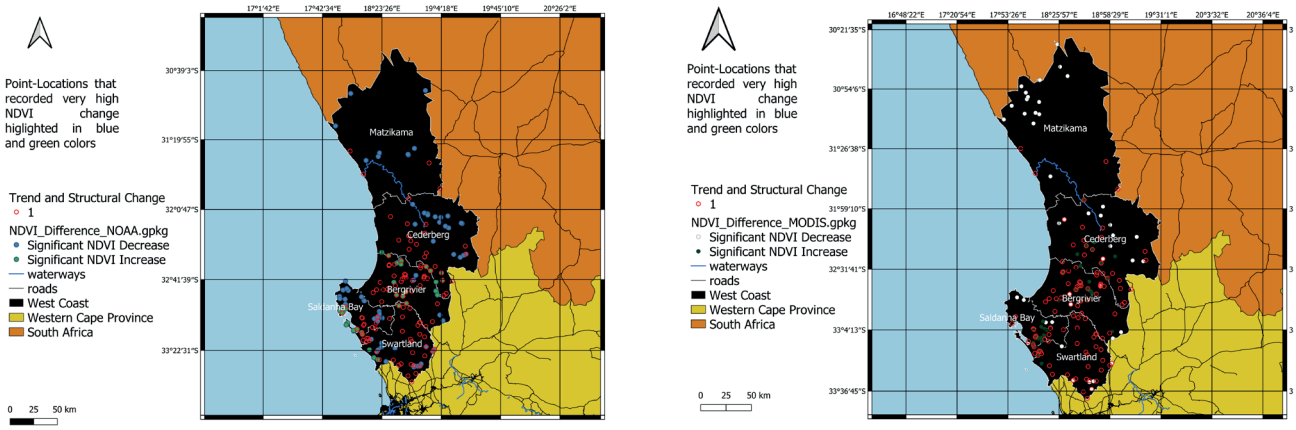

Fig. 15. Point locations that Experienced Significant Land Cover Change over Time

Summary and Conclusions

Land use and land cover (VC) is most probably not a stable or constant phenomenon and ebbs and flows over time. Given the significance and relevance of land use change for economic development and planning and policy formulation, VC change detection becomes very relevant. It therefore seems plausible that the monitoring of VC change dynamics should be instrumental in the effectual planning and sustainable development of expanding economies. To this end, the normalized difference vegetation index (NDVI) is one of the widely accepted methods of classification applied in VC change detection.

The study mainly followed a general to specific approach, specifically with regard to the method of analysis. In terms of the general approach, the focus was on raster and vector (area) analysis applied to the five regions covering the regions as a collective (i.e., the district). The specific approach, on the other hand, focused on point pattern (point-locations) analysis applied to a sample of 100 random points within each Region of interest, i.e., reducing the size of the regions to 100 point-locations each, assuming these point-locations are representative of the regions as a whole.

Two remote sensing datasets were used for this study in both the general and specific approaches. The first dataset was the NOAA CDR AVHRR NDVI: Normalized Difference Vegetation Index, Version 5 dataset. The second dataset was the MOD13Q1.006 Terra Vegetation Indices 16-Day Global 250m dataset. Five municipal areas (regions of interest) were chosen for the study. The regions (district as a collective) are located on the West Coast of South Africa within the Western Cape Province (red boundary). The district accounts for about 2.6 percent and 24 percent of the total land surface of South Africa and the Western Cape Province, respectively.

Temporal differencing the 1981 to 1985, 2015 to 2019, 2000 to 2004, and 2015 to 2020 NOAA and MODIS images respectively yielded images that suggested that the areas that experienced large changes in NDVI values have been random in spatial terms. In general, most of these areas (large change areas) experienced decreases (deterioration) in NDVI values. On the other hand, most areas within each Region only experienced modest decreases (deterioration) in NDVI values. The 500 point-location analysis proposed that many locations within the Swartland, Saldanha Bay and Bergriver regions experienced positive change whilst most locations within the Cederberg and Matzikama regions experienced negative change.

In order to test the NDVI spatial autocorrelation hypothesis the study employed the Global Moran I index. The associated z-values suggested a strong acceptance of the alternative hypothesis of spatial clustering, i.e., presence of spatial autocorrelation. It was noticeable that the Moran I statistics significantly increased during the winter (rain) months irrespective of the dataset. In each case, the Moran I statistics doubled during the winter months. The spatial autocorrelation of the 500 point-locations, therefore, displayed significant seasonal patterns.

Testing for the presence of time relationships utilizing both the cross section independent and cross section dependent unit root testing procedures strongly supported the stationarity hypothesis in that the various

test statistics probability values indicated the acceptance of the alternative hypothesis, i.e., the absence of unit roots. This suggested that the NDVI values of the 500 point-locations were mean reverting over time and therefore no significant structural change has occurred. Applying the Mann-Kendall trend test indicated that the majority of point-locations based on the NOAA time series, MODIS time series and MODIS trend series had not experienced a trend over time.

In the main, areas that recorded significant changes in their NDVI values (plus or minus 0.4 difference on their original NDVI value) over time, in general, have experienced significant and permanent VC change. These areas are also spatially clustered and concentrated within specific areas within the wider district. These areas constitute, however, only a minority of areas (less than 20%), whereas most of the areas within the district did not experience such significant and permanent change in VC. Rather, the changes that did occur in these majority of areas were related to seasonal variation, i.e., temporal changes. It is therefore possible to argue that most of the locations within the district have not experienced any significant and permanent change since the 1980s.

REFERENCES

Anselin L. (1996). The Moran Scatterplot as an ESDA Tool to Assess Local Instability in Spatial Association, in: M. Fischer, H. J. Scholten, D. Unwin (Eds.), Spatial analytical perspectives on GIS. Taylor & Frances, London, England, p. 111–125.

Aburas M.M., Abdullah S.H., Ramli M.F. & Ash'aari Z.H. (2015). Measuring land cover change in Seremban, Malaysia using NDVI index. Procedia Environmental Sciences. 30, 238 – 243.

Alawamy J.S., Balasundram S.K., Mohd. Hanif A.H. & Sung C.T.B. (2020). Detecting and Analyzing Land Use and Land Cover Changes in the Region of Al-Jabal Al-Akhdar, Libya Using Time-Series Landsat Data from 1985 to 2017. Sustainability 2020, 12, 4490 DOI:10.3390/su12114490.

Ahmad I., Tang D., Wang T., Wang M. & Wagan B. (2015). Precipitation trends over time using Mann-Kendall and Spearman's rho tests in Swat River basin, Pakistan. Adv. Meteorol.

Ayele G.T., Tebeje A.M., Demissie S.S., Belete A.M., Jemberrie M.A., Teshome W.M., Mengistu D.T. & Teshale E.Z. (2018). Time Series Land Cover Mapping and Change Detection Analysis Using Geographic Information System and Remote Sensing, Northern Ethiopia. Air, Soil and Water Research, 11, 1–18.

Cihlar J. (2000). Land cover mapping of large areas from satellites: status and research priorities. International Journal of Remote Sensing. 21(6), 1093–1114.

Campos J., Ericsson N.R. & Hendry D.F. (2005). General-to-specific Modeling: An Overview and Selected Bibliography. Board of Governors of the Federal Reserve System, International Finance Discussion Papers, Number 838.

Chang Y. & Song W. (2002). Panel Unit Root Tests in the Presence of Cross-Sectional Dependency and Heterogeneity. Presentation at the 2002 ASSA Meeting held in Atlanta.

Das S. & Angadi D.P. (2020). Land use land cover change detection and monitoring of urban growth using remote sensing and GIS techniques: a micro-level study. GeoJournal, DOI: 10.1007/s10708-020-10359-1.

Deng J., Wang K., Deng Y. & Qi G. (2008). PCA-based landuse change detection and analysis using multispectral and multisensor satellite data. International Journal of Remote Sensing, 29(16), 4823–4838.

Di Gregorio A. & Jansen L.J.M. (2000). Land Cover Classification System (LCCS): Classification Concepts and User Manual. Food and Agriculture Organization of the United Nations, Rome, 1998.

Drapela K. & Drapelova I. (2011). Application of Mann-Kendall test and the Sen's slope estimates for trend detection in deposition data from Bílý Kříž (Beskydy Mts., the Czech Republic) 1997–2010. Beskdy Mendel University in Brno, 4 (2), 133–146.

Firl G.J. & Carter F. (2011). Lesson 10: Calculating Vegetation Indices from Landsat 5 TM and Landsat 7 ETM+ Data. [online] Available at: http://ibis.colostate.edu/webcontent/ws/coloradoview/tutorialsdownloads/co_rs_tutorial10.pdf. [Accessed 15 May 2021]

Google Earth Engine, Gorelick N., Hancher M., Dixon M., Ilyushchenko S., Thau D., & Moore R. (2017). Google Earth Engine: Planetary-scale geospatial analysis for everyone. Remote Sensing of Environment.

Herwartz H. (2007). A note on model selection in (time series) regression models - General-to-specific or specific-to-general?. Economics Working Paper, 2007-09.

De Jong R. & Sakarya H. (2016). The Econometrics of the Hodrick-Prescott Filter. The Review of Economics and Statistics. 98(2), 310–317.

Le Roux A., Cooper A.K. & Mans G. (2016). Land Use and Land Cover Change in the Western Cape Province: Quantification of Changes & Understanding of Driving Factors. Conference: 7th Planning Africa Conference 2016 – Making Sense of the Future: Disruption and Reinvention At: Johannesburg, South Africa

Meals D.W., Spooner J., Dressing S.A. & Harcum J.B. (2011). Statistical analysis for monotonic trends. Tech Notes 6, November 2011. Developed for U.S. Environmental Protection Agency by Tetra Tech, Inc., Fairfax, VA, 23.

Meneses-Tovar C. (2012). NDVI as indicator of degradation. Unasylva (FAO).

MODIS (2021). Images and data from 2000 was retrieved on 2021/01/10 from https://lpdaac.usgs.gov, maintained by the NASA EOSDIS Land Processes Distributed Active Archive Center (LP DAAC) at the USGS Earth Resources Observation and Science (EROS) Center, Sioux Falls, South Dakota. 2018.

Mucina L., Knevel I.C., Adams J.B. & Rutherford M.C. (2006). Coastal Vegetation of South Africa. Strelitzia 19(2006)

Mbatha N. & Xulu S. (2018). Time Series Analysis of MODIS-Derived NDVI for the Hluhluwe-Imfolozi Park, South Africa: Impact of Recent Intense Drought. Climate, 6, 95, DOI:10.3390/cli6040095.

NOAA (2021). NOAA Climate Data Record (CDR) of AVHRR Normalized Difference Vegetation Index (NDVI), v5. [online] Available at: https://data.noaa.gov/dataset/dataset/noaa-climate-data-record-cdr-of-avhrr-normalized-difference-vegetation-index-ndvi-version-5. [Accessed 15 May 2021]

Motiee H. & McBean E. (2009). An Assessment of Long Term Trends in Hydrologic

Components and Implications for Water Levels in Lake Superior. Hydrology Research, 40(6), 564-579.

Rogan J. & Chen D. (2004). Remote sensing technology for mapping and monitoring land-cover and land-use change. Progress in Planning. 61(4), 301-325.

Rouse J. W., Haas R. H., Schell J. A. & Deering D. W. (1974). Monitoring vegetation systems in the Great Plains with ERTS. NASA. Goddard Space Flight Center 3d ERTS-1 Symp., 1, Sect. A

Sahebjalal E. & Dashtekian K. (2013). Analysis of land use-land covers changes using normalized difference vegetation index (NDVI) differencing and classification methods. African Journal of Agricultural Research, 8(37), 4614-4622.

Sowunmi F. A., Akinyosoye V. O., Okoruwa V.O. & Omonona B. T. (2012). The Landscape of Poverty in Nigeria: A Spatial Analysis Using Senatorial Districts- level Data. American Journal of Economics. 2(5), 61–74.

Vermote E., Justice C., Csiszar I., Eidenshink J., Myneni R., Baret F., Masuoka E., Wolfe R., Claverie M. & NOAA CDR Program (2014): NOAA Climate Data Record (CDR) of Normalized Difference Vegetation Index (NDVI), v4. [indicate subset used]. NOAA National Climatic Data Center. DOI:10.7289/V5PZ56R6.

Viton P. A. (2010). Notes on Spatial Econometric Models. City and Regional Planning, 870(3):2-17.

Wade T.G., Wickham J.D., Nash M. & Neale A.C. (2003). A Comparison of Vector and Raster GIS Methods for Calculating Landscape Metrics Used in Environmental Assessments. Photogrammetric Engineering and Remote Sensing. 69(12), 1399–1405.

Wu D.H., Zhao X., Liang S.L., Zhou T., Huang K.C., Tang B.J. & Zhao W.Q. (2015). Time-lag effects of global vegetation responses to climate change. Global Chang. Biol, DOI:10.1111/gcb.12945.

Yue S. & Wang C. (2004). The Mann-Kendall Test Modified by Effective Sample Size to Detect Trend in Serially Correlated Hydrological Series. Water Resources Management, 18, 201–218.

Zhang B.Q., Wu P., Zhao X.N., Wang Y.B. & Gao X.D. (2013). Changes in vegetation condition in areas with different gradients (1980–2010) on the Loess Plateau, China. Environ. Earth Sci, 68, 2427–2438.

Zhao G., Lin G., & Warner T. (2004). Thematic mapper data for change detection and sustainable use of cultivated land: A case study in the Yellow River delta. China. International Journal of Remote Sensing, 25(13), 2509–2522.